
Rethinking the Implementation Matters in Cooperative Multi-Agent Reinforcement Learning

Jian Hu ^{*†}

Graduate Institute of Networking and Multimedia
National Taiwan University
Taipei
r08944053@ntu.edu.tw

Siyang Jiang ^{*}

Graduate Institute of Electrical Engineering
National Taiwan University
Taipei
syjiang@arbor.ee.ntu.edu.tw

Seth Austin Harding

Department of Computer Science
National Taiwan University
Taipei
b06902101@ntu.edu.tw

Haibin Wu

Graduate Institute of Communication Engineering
National Taiwan University
Taipei
f07921092@ntu.edu.tw

Shih-wei Liao

Department of Computer Science
National Taiwan University
Taipei
liao@csie.ntu.edu.tw

Abstract

Multi-Agent Reinforcement Learning (MARL) has seen revolutionary breakthroughs with its successful application to multi-agent cooperative tasks such as computer games and robot swarms. QMIX, a widely popular MARL algorithm, has been used to solve cooperative tasks, e.g. Starcraft Multi-Agent Challenge (SMAC), Difficulty-Enhanced Predator-Prey (DEPP). Recent variants of QMIX target relaxing the monotonicity constraint of QMIX, allowing for performance improvement in SMAC. However, in this paper, we investigate the code-level optimizations of these variants and the monotonicity constraint. We find that (1) such improvements of the variants are significantly affected by various code-level optimizations; (2) QMIX with normalized optimizations outperforms other previous works in SMAC; (3) the monotonicity constraint may improve sample efficiency in SMAC and DEPP. Last, a discussion with theoretical analysis is demonstrated about why QMIX works well in SMAC. We open-source the code at <https://github.com/hijkzzz/pymarl2>

1 Introduction

Multi-agent cooperative games have many complex real-world applications such as autonomous vehicle coordination [3], robot swarm control [7] and sensor networks [36]. Multi-Agent Reinforcement Learning (MARL) has broad prospects for addressing such cooperative tasks [23; 31]. As there is limited scalability and inherent constraints on agent observability and communication in many multi-agent environments, decentralized policies that act only on their local observations

^{*} Jian Hu and Siyang Jiang contributed equally to this work.

[†] Corresponding author.

are necessitated and widely used [37]. Learning decentralized policies is an intuitive approach for training agents independently. However, simultaneous exploration by multiple agents often results in non-stationary environments, which leads to unstable learning. Therefore, *Centralized Training and Decentralized Execution* (CTDE) [9] allows for independent agents to access additional state information that is unavailable during policy inference.

Many CTDE learning algorithms have been proposed for multi-agent cooperative tasks[34], among which several value-based approaches achieve state-of-the-art (SOTA) performance [18; 30; 35; 19] on such tasks, e.g., Starcraft Multi-Agent Challenge (SMAC) [20], Predator-Prey (PP) [10], Difficulty-Enhanced Predator-Prey (DEPP) [2; 15]. To enable effective CTDE for multi-agent Q-learning, the Individual-Global-Max (IGM) principle [22] of equivalence of joint greedy action and individual greedy actions is critical. The primary advantage of the IGM principle is that it ensures consistency of policy with centralized training and decentralized execution. To enable this principle, a value-based method, QMIX [18], was proposed for factorizing the joint action-value function with the *Monotonicity Constraint* [30], limiting the the expressive power of the mixing network.

To generalize and improve the performance of QMIX, some variants of QMIX ³, including value-based approaches [35; 19; 30; 23] and a policy-based approach [37], have been proposed with the aim to relax the monotonicity constraint of QMIX. However, while investigating the codes of these variants, we find that their performance is significantly affected by their code-level optimizations. Therefore, it is left unclear whether monotonicity constraint indeed impairs the QMIX’s performance.

In this paper, we investigate the impact of the *code-level optimizations* and the *monotonicity constraint* in multi-agent purely cooperative tasks. Firstly, to explore the effects of code-level optimizations, we perform an ablation analysis in SMAC. Afterwards, we normalize the optimizations of QMIX and its variants; specifically, we perform the same hyperparameter search pattern for all algorithms, which includes using or removing a certain optimization and a grid hyperparameter search. Under the normalized settings, our experiment results (Sec. 5.2.1) demonstrate that QMIX outperforms other variants, becoming the SOTA ⁴. Secondly, to study the impact of the monotonicity constraint, we propose a policy-based algorithm, RIIT; the experimental results (Sec. 5.2.2) show that the monotonicity constraint improves sample efficiency in SMAC and DEPP. Lastly, to generalize cooperative tasks beyond SMAC and DEPP, we give a strict definition of purely cooperative tasks, and discuss why QMIX works well in purely cooperative tasks with a theoretical analysis.

To our best knowledge, this work is the first to analyze the monotonicity constraint, and we believe that this work will help the community understand theses approaches.

2 Preliminaries

Dec-POMDP. A decentralized partially observable Markov decision process (Dec-POMDP) [14] composed of a tuple $G = \langle \mathcal{S}, \mathcal{U}, P, r, \mathcal{Z}, O, N, \gamma \rangle$. $s \in \mathcal{S}$ describes the true state of the environment. At each time step, each agent $i \in \mathcal{N} := \{1, \dots, N\}$ chooses an action $u^i \in \mathcal{U}$, forming a joint action $\mathbf{u} \in \mathcal{U}^N$. All state transition dynamics are defined by function $P(s' | s, \mathbf{u}) : \mathcal{S} \times \mathcal{U}^N \times \mathcal{S} \mapsto [0, 1]$. Each agent has independent observation $z \in \mathcal{Z}$, determined by observation function $O(s, i) : \mathcal{S} \times \mathcal{N} \mapsto \mathcal{Z}$. All agents share the same reward function $r(s, \mathbf{u}) : \mathcal{S} \times \mathcal{U}^N \rightarrow \mathbb{R}$ and $\gamma \in [0, 1]$ is the discount factor. The objective function, shown in Eq. 1, is to maximize the joint value function to find a joint policy $\pi = \langle \pi_1, \dots, \pi_n \rangle$.

$$J(\pi) = \mathbb{E}_{u^1 \sim \pi^1, \dots, u^N \sim \pi^N, s \sim \mathcal{S}} \left[\sum_{t=0}^{\infty} \gamma^t r_t(s_t, u_t^1, \dots, u_t^N) \right] \quad (1)$$

Centralized Training and Decentralized Execution (CTDE). CTDE is a popular paradigm [30] which allows for the learning process to utilize additional state information [9]. Agents are trained in a centralized way, i.e., learning algorithms, to access all local action observation histograms, global states, and sharing gradients and parameters. In the execution stage, each individual agent can only access its local action observation history τ^i .

³These algorithms are based on the mixing network from QMIX, so we call the variants of QMIX.

⁴Note that the result also demonstrates the impact of the monotonicity constraint; we echo this view in Sec. 5.2.1.

QMIX and Monotonicity Constraint. To resolve the credit assignment problem in multi-agent learning, QMIX [18] learns a joint action-value function Q_{tot} which can be represented in Eq. 2:

$$\begin{aligned} Q_{tot}(s, u; \theta, \phi) &= g_\phi(s, Q_1(\tau^1, u^1; \theta^1), \dots, Q_N(\tau^N, u^N; \theta^N)) \\ \frac{\partial Q_{tot}(s, u; \theta, \phi)}{\partial Q_i(\tau^i, u^i; \theta^i)} &\geq 0, \quad \forall i \in \mathcal{N} \end{aligned} \quad (2)$$

where ϕ is the trainable parameter of the monotonic mixing network, which is a mixing network with monotonicity constraint, and θ^i is the parameter of the agent network i . Benefiting from the monotonicity constraint in Eq. 2, maximizing joint Q_{tot} is precisely the equivalent of maximizing individual Q_i , resulting in and allowing for optimal individual action to maintain consistency with optimal joint action. QMIX learns by sampling a multitude of transitions from the replay buffer and minimizing the mean squared temporal-difference (TD) error loss:

$$\mathcal{L}(\theta) = \frac{1}{2} \sum_{i=1}^b \left[(y_i - Q_{tot}(s, u; \theta, \phi))^2 \right] \quad (3)$$

where the TD target value $y = r + \gamma \max_{u'} Q_{tot}(s', u'; \theta^-, \phi^-)$ and θ^-, ϕ^- are the target network parameters copied periodically from the current network and kept constant for a number of iterations. However, the monotonicity constraint limits the mixing network's expressiveness, which may fail to

12	-12	-12
-12	0	0
-12	0	0

(a) Payoff matrix

-12	-12	-12
-12	0	0
-12	0	0

(b) QMIX: Q_{tot}

Table 1: A non-monotonic matrix game. Bold text indicates the reward of the argmax action.

learn in non-monotonic cases [11] [19]. Table 1a shows a non-monotonic matrix game that violates the monotonicity constraint. This game requires both agents to select the first action 0 (actions are indexed from top to bottom, left to right) in order to catch the reward 12; if only one agent selects action 0, the reward is -12. QMIX may learn an incorrect Q_{tot} which has an incorrect argmax action as shown in Table 1b.

3 Related Works

In this section, we describe the variants of QMIX and investigate various code-level optimization works. We explain the details of these algorithms and show the code resources in Appendix E.

Value-based Methods To enhance the expressive power of QMIX, Qatten [35] introduces an attention mechanism to enhance the expression of QMIX; QPLEX [30] transfers the monotonicity constraint from Q values to Advantage values [13]; QTRAN++ [23] and WQMIX [19] further relax the monotonicity constraint through a true value network and some theoretical constraints; however, Value-Decomposition Networks (VDNs) [27] only requires a linear decomposition where $Q_{tot} = \sum_i^N Q_i$, which can be seen as strengthening monotonicity constraint .

Policy-based Methods LICA [37] completely removes the monotonicity constraint through a policy mixing critic. For other MARL policy-based methods, VMIX [25] combines the Advantage Actor-Critic (A2C) [24] with QMIX to extend the monotonicity constraint to value networks, i.e., replacing the value network with the monotonic mixing network. DOP [32] learns the policy networks using the Counterfactual Multi-Agent Policy Gradients (COMA) [6] with the Q_i decomposed by QMIX.

Code-level Optimizations Engstrom *et.al* [5] investigates code-level optimizations based on PPO [21] implementation, and concludes that the majority of performance differences between PPO and TRPO originate from code-level optimizations. Andrychowicz *et. al* [1] investigates the influence of code-level optimizations on the performance of PPO and provides tuning optimizations.

4 Experiments Setup

4.1 Benchmark Environment

SMAC is used as our main benchmark testing environment, which is a ubiquitously-used multi-agent discrete cooperative control environment for MARL algorithms [30; 18; 23; 19]. SMAC consists of a set of StarCraft II micro scenarios used for evaluating the effectiveness of independent agents in coordinating to solve complicated tasks, and it classifies micro scenarios into three difficulty levels: Easy, Hard, and Super Hard. The simplest VDNs [27] are usually used to effectively solve the Easy scenarios. It is worth noting that QMIX and VDNs achieves a 0% win rate in three Super Hard scenarios *corridor*, *3s5z_vs_3s5z*, and *6h_vs_8z* in past SMAC experiments [20]. Therefore, we only investigate the Hard and Super Hard scenarios in SMAC.

Difficulty-Enhanced Predator-Prey (DEPP) In vanilla Predator-Prey (PP) [10], three cooperating agents control three predators to chase a faster prey (the prey acts randomly). The goal is to capture the prey with the fewest steps possible. We leverage two difficulty-enhanced Predator-Prey variants to test the algorithms. (1) The first variant of Predator-Prey [2] requires two predators to catch the prey at the same time to get a reward. (2) In the Continuous Predator-Prey [15], the prey’s policy is replaced by a hard-coded heuristic, i.e., at any time step, moving the prey to the sampled position with the largest distance to the closest predator.

4.2 Evaluation Metric

Our primary evaluation metric is the function that maps the steps for the environment observed throughout the training to the median winning percentage (episode return for Predator-Prey) of the evaluation. Just as in QMIX [18], we repeat each experiment with several independent training runs (five independent random experiments). In order to accurately evaluate the convergence performance of each algorithm, eight rollout processes for parallel sampling are used to obtain as many samples as possible from the environments at a high rate⁵.

5 Experiments

Our experiments consist of two parts⁶. The first part demonstrates the performance of several isolated tricks from the variants. The second part is the reconceptualization of the monotonicity constraint.

5.1 Code-level Optimizations

The code-level optimizations are the tricks unaccounted for in the experimental design, but that might hold significant effects on the result. To better understand their influences on performance, we perform ablation experiments on these tricks incrementally and provide some suggestions for tuning.

5.1.1 Optimizer

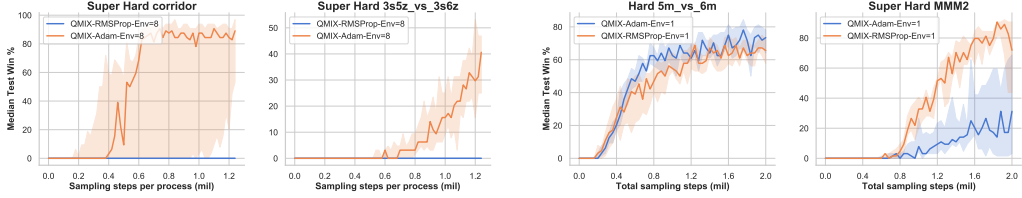
Study description. QMIX and the majority of its variant algorithms use RMSProp to optimize neural networks as they prove stable in SMAC. We attempt to use Adam to optimize QMIX’s neural network with quickly convergence benefiting from momentum:

Interpretation. Figure 1a shows that Adam [8] increases the win rate by 100% on the Super Hard map *corridor*. Adam boosts the network’s convergence allowing for full utilization of the large quantity of samples sampled in parallel. However, Figure 1b shows that when we use only one sampling process, samples are updated slower than with eight processes (the replay buffer size is fixed), and the neural network becomes prone to overfitting. We find that the Adam optimizer solves the problem posed by [25] in which QMIX does not work well under parallel training.

Recommendation. Use Adam and quickly update the samples.

⁵Our experiments can collect 10 million samples within 9 hours with a Core i7-7820X CPU and a GTX 1080 Ti GPU.

⁶Note that our experimental results are not directly comparable with the previous work, as we use StarCraft 2 (SC2.4.10) in the latest PyMARL.



(a) Eight rollout processes are used for sampling.

(b) Only one rollout process is used for sampling.

Figure 1: (a) Adam significantly improves performance when samples are updated quickly; (b) The Q networks optimized by Adam is prone to overfitting when samples are updated slowly.

5.1.2 Eligibility Traces

Study description. Eligibility traces such as $\text{TD}(\lambda)$ [28], $\text{Q}(\lambda)$ [16], and $\text{TB}(\lambda)$ [17] achieve a balance between return-based algorithms (where return refers to the sum of discounted rewards $\sum_t \gamma^t r_t$) and bootstrap algorithms (where return refers to $r_t + V(s_{t+1})$), speeding up the convergence of reinforcement learning algorithms. Therefore, we study the application of $\text{Q}(\lambda)$ ⁷ in QMIX.

Interpretation. Q networks without sufficient training usually have a large bias that impacts bootstrap returns. Figure 2a shows that $\text{Q}(\lambda)$ allows for faster convergence in our experiments by reducing this bias. However, large values of λ may lead to failed convergence due to variance and off-policy bias. Figure 2a shows that when λ is set to 0.9, it has a detrimental impact on the performance of QMIX.

Recommendation. Use $\text{Q}(\lambda)$ with a small value of λ .

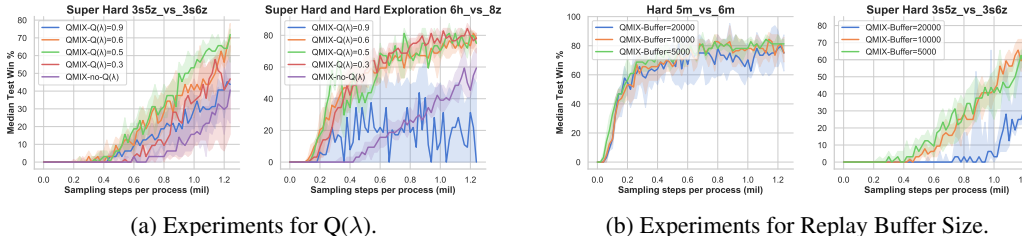


Figure 2: (a) $\text{Q}(\lambda)$ significantly improves performance of QMIX, but large values of λ lead to instability in the algorithm. (b) Setting the replay buffer size to 5000 episodes allows for QMIX’s learning to be more stable than by setting it to 20000 episodes.

5.1.3 Replay Buffer Size

Study description. In single-agent Deep Q-networks (DQN), the replay buffer size is usually set to a large value. However, in multi-agent tasks, as the action space becomes larger than that of single-agent tasks, the distribution of samples changes more quickly. In this section, we study the impact of the replay buffer size on performance.

Interpretation. Figure 2b shows that a large replay buffer size causes instability in QMIX’s learning. The causes of this phenomenon are as follows: (1) In multi-agent tasks, samples become obsolete more quickly than in single-agent tasks. (2) Echoing in Sec. 5.1.1, Adam performs better with samples with fast updates. (3) When the sampling policy is far from the current policy, the return-based methods require importance sampling ratios, which is difficult to calculate in multi-agent learning.

Recommendation. Use a small replay buffer size.

5.1.4 Rollout Process Number

Study description. When we collect samples in parallel as is done in A2C [24], it shows that when there is a defined total number of samples and an unspecified number of rollout processes, the median

⁷We explain the formula of $\text{Q}(\lambda)$ in Appendix B.

test performance becomes inconsistent. This study aims to perform analysis and provide insight on the impact of the number of processes on the final performance.

Interpretation. Under the A2C [13] training paradigm, the total number of samples can be calculated as $S = E \cdot P \cdot I$, where S is the total number of samples, E is the number of samples in each episode, P is the number of rollout processes, and I is the number of policy iterations. Figure 3a shows that we are given both S and E ; the fewer the number of rollout processes, the greater the number of policy iterations [28]; a higher number of policy iterations leads to an increase in performance. However, it also causes both longer training time and decreased stability.

Recommendation. Use fewer rollout processes when samples are difficult to obtain; otherwise, use more rollout processes.



Figure 3: (a) Given the total number of samples, fewer processes achieve better performance. We set the replay buffer size to be proportional to the number of processes to ensure that the novelty of the samples is consistent. (b) On the $6h_vs_8z$, defining a proper length for ϵ anneal period significantly improves performance.

5.1.5 Exploration Steps

Study description. Some scenarios in SMAC are hard to explore, such as $6h_vs_8z$, so the settings of ϵ -greedy become critically important. In this study, we analyze the effect of ϵ anneal period on performance.

Interpretation. As shown in Figure 3b, increasing the length of the ϵ anneal period from 100K steps to 500K steps allows for a 38% increase in win rate in the Super Hard Exploration scenario $6h_vs_8z$. However, increasing this value to 1000K instead causes the model to collapse.

Recommendation. Increase the value of the ϵ anneal period to an appropriate length on hard-to-explore scenarios.

5.1.6 Bonus: Rewards Shaping

Study description. Table 1a shows a non-monotonic case that QMIX cannot solve. However, the reward function in MARL is defined by the user; we investigate whether QMIX can learn a correct argmax action by reshaping the task’s reward function without changing its goal.

12.0	-0.5	-0.5
-0.5	0	0
-0.5	0	0

(a) Reshaped Payoff matrix

12.0	-0.3	-0.3
-0.3	-0.3	-0.3
-0.3	-0.3	-0.3

(b) QMIX: Q_{tot}

Table 2: A non-monotonic matrix game in which we reshape the reward by replacing the insignificant reward -12 (in Table 1a) with reward -0.5. QMIX learns a Q_{tot} which has a correct argmax. Bold text indicates argmax action’s reward.

Interpretation. The reward -12 in Table 1a does not assist the agents in finding the optimal solution; as shown in Table 2, this non-monotonic matrix may be solved by simply replacing the insignificant reward -12 with -0.5. The reward shaping may also help QMIX learn more effectively in other non-monotonic tasks.

Recommendation. Increase the scale of the important rewards of the tasks and reduce the scale of rewards that may cause disruption.

5.2 Rethinking of the Monotonicity Constraint

In this subsection, we first present the performance improvement of QMIX with all the above optimizations. Note that *Reward Shaping* is not added since SMAC provides a default setting for a shaped reward. In addition, we normalize the optimizations for all algorithms, i.e., the same hyperparameter search pattern is used for all algorithms, which includes whether we use a certain optimization as well as a grid search for these hyperparameters (details in Appendix D). We denote the optimized algorithms with the prefix *Our*. Second, ablation studies are demonstrated to further study the effects of the monotonicity constraint.

5.2.1 QMIX with Normalized Tricks

Scenarios	Difficulty	QMIX	OurQMIX
5m_vs_6m	Hard	84%	90%
3s_vs_5z	Hard	96%	100%
bane_vs_bane	Hard	100%	100%
2c_vs_64zg	Hard	100%	100%
corridor	Super Hard	0%	100%
MMM2	Super Hard	98%	100%
3s5z_vs_3s6z	Super Hard	3%	85% (Number of Envs = 4)
27m_vs_30m	Super Hard	56%	100%
6h_vs_8z	Super Hard	0%	93% ($\lambda = 0.3$)

Table 3: Best test results of OurQMIX and vanilla QMIX in all hard scenarios.

As shown in Table 3, OurQMIX attains higher win rates in all hard and super hard SMAC scenarios, far exceeding vanilla QMIX. The result shows that the code-level optimizations are vital for better performance. As shown in Table 4⁸, the test results on the hardest scenarios in SMAC and DEPP demonstrate that **(I)** The performance of OurVDNs, OurQatten, OurQPLEX, OurWQMIX exceeds the test results in the past literatures [20; 30; 15; 19](details in Appendix D.3). **(II)** The linear OurVDNs is also relatively effective (6h_vs_8z). **(III)** When the sample size is reduced from 64 million used by LICA [37] to 10 million, LICA has terrible performance. **(IV)** OurQMIX achieves SOTA. **(V)** We notice that the performance of the algorithm becomes progressively worse as the monotonicity constraint decreases (QMIX > QPLEX > WQMIX > LICA) in the benchmark environment⁹.

The experimental results, specifically **(II)**, **(IV)**, **(V)**, show that these variants of QMIX that relax the monotonicity constraint do not obtain better performance than QMIX in either SMAC or DEPP.

5.2.2 Ablation Studies of Monotonicity Constraint

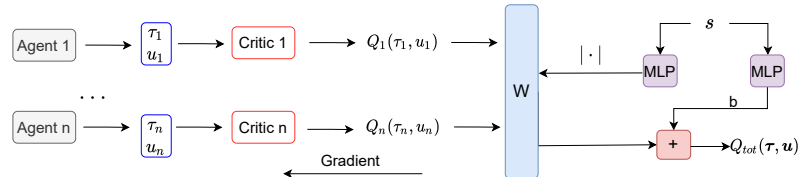


Figure 4: Architecture for RIIT: $|\cdot|$ denotes absolute value operation, implementing the monotonicity constraint of QMIX. W denotes the non-negative mixing weights. Agent i denotes the policy network which can be trained end-to-end by maximizing the Q_{tot} .

We further study the impact of monotonicity constraint tasks via comparing the performance of adding or removing the constraint. An end-to-end Actor-Critic method, RIIT, is proposed. Note that

⁸We also avoid using the optimal hyperparameters of QMIX for comparison, so the experimental results of QMIX in Table 3 are different from those found in 4, and we also compare the performance between *Our* and the original methods in Appendix D.3 due to the page limitation.

⁹We explain this inequality in detail in E.8 due to the page limitation.

Algo.	Type	MNS	5m_vs_6m	3s5z_vs_3s6z	corridor	6h_vs_8z	MMM2	PP
OurQMIX	VB	41K	90%	75%	100%	84%	100%	40
OurVDNs	VB	0K	90%	43%	98%	87%	96%	39
OurQatten	VB	58K	90%	62%	100%	68%	100%	-
OurQPLEX	VB	152K	90%	68%	96%	78%	100%	39
OurWQMIX	VB	247K	90%	6%	96%	78%	23%	39
OurLICA	PG	208K	53%	0%	0%	4%	0%	30
OurDOP	PG	122K	9%	0%	0%	1%	0%	32
RIIT	PG	69K	67%	75%	100%	19%	100%	38

Table 4: Median test win rate (episode return) of QMIX-based algorithms with normalized tricks. PG denotes Policy-gradient; VB denotes Value-based; PP denotes Predator Prey. The Mixing Net Size (MNS) is calculated under *6h_vs_8z*.

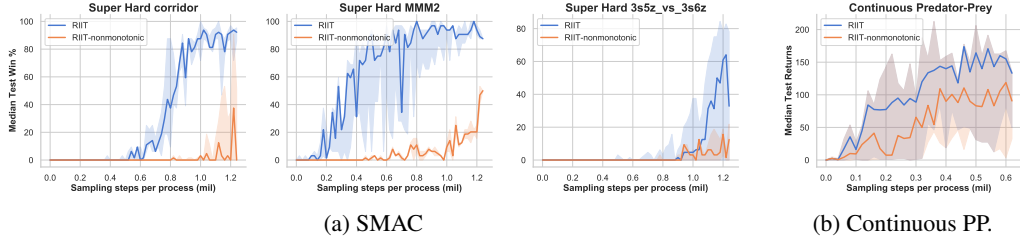


Figure 5: Comparing RIIT w./ and w/o. monotonicity constraint (remove absolute value operation) on SMAC (a) and Continuous Predator-Prey (b).

RIIT is not our main contribution, and it can be seen as a method to study the effects of monotonicity constraint. Specifically, we use the monotonic mixing network as a critic network, shown in Figure 4. Then, in Eq. 4, with a trained critic $Q_{\theta_c}^{\pi}$ estimate, the decentralized policy networks $\pi_{\theta_i}^i$ can then be optimized end-to-end simultaneously by maximizing $Q_{\theta_c}^{\pi}$ with the policies $\pi_{\theta_i}^i$ as inputs. Since RIIT is trained end-to-end, it may also be used for continuous control tasks. It is worth stating that the item $\mathbb{E}_i [\mathcal{H}(\pi_{\theta_i}^i(\cdot | z_t^i))]$ is the Adaptive Entropy [37], and we use a two-stage approach to train the actor-critic network, described in detail in Appendix C.

$$\max_{\theta} \mathbb{E}_{t, s_t, u_t^1, \dots, \tau_t^n} [Q_{\theta_c}^{\pi} (s_t, \pi_{\theta_1}^1 (\cdot | \tau_t^1), \dots, \pi_{\theta_n}^n (\cdot | \tau_t^n)) + \mathbb{E}_i [\mathcal{H}(\pi_{\theta_i}^i(\cdot | \tau_t^i))]] \quad (4)$$

The monotonicity constraint on the critic (Figure 4) is theoretically no longer required as the critic is not used for greedy action selection. We can evaluate the effects of the monotonicity constraint by removing the absolute value operation in the monotonic mixing network. In this way, RIIT can also be easily extended to non-monotonic tasks. Figure 5a and Figure 5b demonstrate that the monotonicity constraint significantly improves the performance of RIIT. Table 4 also presents that RIIT performs best among all policy-based multi-agent algorithms.

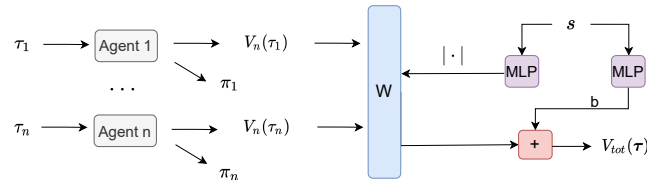


Figure 6: Architecture for VMIX: $|\cdot|$ denotes absolute value operation, decomposing V_{tot} into V_i .

To explore the generality of monotonicity constraints, we extend the above experiments to VMIX [26]. As shown in Figure 6, VMIX adds the monotonicity constraint to the value network (not Q value networks) of A2C. VMIX learns the policy of each agent by advantage-based policy gradient [13]; therefore, the monotonicity constraint is not necessary for greedy action selection either. We can evaluate the effects of the monotonicity constraint by removing the absolute value operation in Figure 6. The result from Figure 7 shows that the monotonicity constraint improves the sample efficiency in value networks. All the test results above indicate that the monotonicity constraint can improve the sample efficiency in SMAC and DEPP.

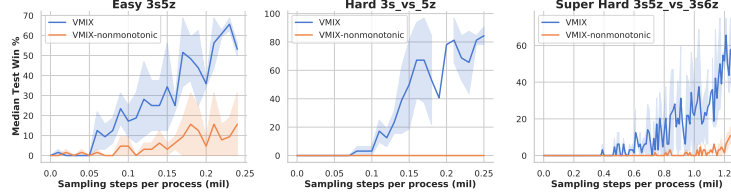


Figure 7: Comparing VMIX with and without monotonicity constraint on SMAC.

6 Discussion

To better understand the monotonicity constraint, we discuss the following two questions with theoretical analysis. **Ques.1** Why can SMAC be represented well by monotonic mixing networks? **Ques.2** Why can the monotonicity constraint improve the sample efficiency in SMAC? To coherently answer the above questions, we give the following definitions and propositions. It is worth noting that the core assumption is that the joint action-value function Q_{tot} can be represented by a non-linear mapping $f_\phi(s; Q_1, Q_2, \dots, Q_N)$, but without the monotonicity constraint.

Definition 1. Cooperative tasks. For a task with N agents ($N > 1$), all agents have a common goal.

Definition 2. Semi-cooperative Tasks. Given a cooperative task with a set of agents \mathbb{N} . For all states s of the task, if there is a subset $\mathbb{K} \subseteq \mathbb{N}$, $\mathbb{K} \neq \emptyset$, where the $Q_i, i \in \mathbb{K}$ increases while the other $Q_j, j \notin \mathbb{K}$ are fixed, this will lead to an increase in Q_{tot} .

As a counterexample, the collective action problem (social dilemma) is not Semi-cooperative task. i.e., since the Q value may not include future rewards when $\gamma < 1$, the collective interest in the present may be detrimental to the future interest.

Definition 3. Competitive. Given two agents i and j , we say that agents i and j are competitive if either an increase in Q_i leads to a decrease in Q_j or an increase in Q_j leads to a decrease in Q_i .

Definition 4. Purely Cooperative Tasks. Semi-cooperative tasks without competitive cases.

Proposition 1. Purely Cooperative Tasks can be represented by monotonic mixing networks.

Proof. Since the QMIX’s mixing network is a universal function approximator of monotonic functions, for a Semi cooperative task, if there is a case (state s) that cannot be represented by a monotonic mixing network, i.e., $\frac{\partial Q_{tot}(s)}{\partial Q_i} < 0$, then an increase in Q_i must lead to a decrease in $Q_j, j \neq i$ (since there is no Q_j decrease, by Def. 2, the constraint $\frac{\partial Q_{tot}(s)}{\partial Q_i} < 0$ does not hold). Therefore, by Def. 3 this cooperative task has a competitive case which means it is not a purely cooperative task. \square

For answering Ques.1: According to the Proposition 1, we need to explain why SMAC is a purely cooperative task environment. SMAC mainly uses a shaped reward signal calculated from the hit-point damage dealt, some positive reward after having enemy units killed and a positive bonus for winning the battle; the reward setting can be interpreted as purely cooperative. In practice, we can decompose the hit-point damage dealt linearly and divide the units killed rewards and victory rewards to the agents near the enemy (last enemy for victory) evenly. The approximate linear decomposition¹⁰ also explains why the VDNs also work well in SMAC (Table. 4).

For answering Ques.2: It is obvious that the monotonicity constraint significantly reduces the hypothesis space of the mixing network¹¹. Note that the Q value decomposition mapping of the SMAC is a subset of the hypothesis space of QMIX. Therefore, using the monotonicity constraint can allow for avoiding searching invalid parameters, leading to a significant improvement in sampling efficiency.

¹⁰As $Q_\pi(s, u) = \mathbb{E}_\pi[\sum_{k=0}^{\infty} \gamma^k r_{t+k+1} \mid s, u]$, the reward is linearly assignable meaning that Q value is linearly assignable.

¹¹Just as in QMIX’s implementation where the monotonicity constraint reduces the range of values of each weight (W in Figure 4) by half, the network’s hypothesis space is assumed to decrease exponentially by $\frac{1}{2}^N$ (N denotes the number of weights).

7 Conclusion

In this paper, we investigate the influence of certain code-level optimizations on the performance of QMIX and provide tuning optimizations. Moreover, we find that relaxing the monotonicity constraint of the mixing network will not always improve the performance of QMIX. i.e, our experiments and analysis demonstrate that the monotonicity constraint can improve the sample efficiency in SMAC. In addition, we discuss why QMIX works well in purely cooperative tasks. We believe that the variants of QMIX that relax monotonicity constraint may be well-suited for the nonmonotonic environment, such as cooperative tasks with competition.

8 Broader Impact

Many complex real-world problems can be formulated as multi-agent cooperative games. For example, decentralized agents can be applied to robot swarm control, vehicle coordination, and network routing. Applying MARL to these scenarios often requires a large number of samples to train the model, which implies high costs, such as thousands of CPUs, power resources, and expensive robotic equipment. Taking into consideration our carbon footprint, there is an urgent need to avoid any and all waste of resources. The monotonicity constraint of QMIX helps to improve the sample efficiency in some hard purely cooperative tasks, thereby reducing wasting of resources.

References

- [1] Marcin Andrychowicz, Anton Raichuk, Piotr Stańczyk, Manu Orsini, Sertan Girgin, Raphael Marinier, Léonard Hussenot, Matthieu Geist, Olivier Pietquin, Marcin Michalski, Sylvain Gelly, and Olivier Bachem. What Matters In On-Policy Reinforcement Learning? A Large-Scale Empirical Study. *arXiv:2006.05990*, 2020.
- [2] Wendelin Böhmer, Vitaly Kurin, and Shimon Whiteson. Deep coordination graphs. In *International Conference on Machine Learning*, 2020. URL <https://arxiv.org/abs/1910.00091>.
- [3] Yongcan Cao, Wenwu Yu, Wei Ren, and Guanrong Chen. An overview of recent progress in the study of distributed multi-agent coordination. *IEEE Transactions on Industrial informatics*, 9(1):427–438, 2012.
- [4] Karl Cobbe, Jacob Hilton, Oleg Klimov, and John Schulman. Phasic policy gradient. *arXiv preprint arXiv:2009.04416*, 2020.
- [5] Logan Engstrom, Andrew Ilyas, Shibani Santurkar, Dimitris Tsipras, Firdaus Janoos, Larry Rudolph, and Aleksander Madry. Implementation Matters in Deep Policy Gradients: A Case Study on PPO and TRPO. *arXiv:2005.12729*, 2020.
- [6] Jakob Foerster, Gregory Farquhar, Triantafyllos Afouras, Nantas Nardelli, and Shimon Whiteson. Counterfactual Multi-Agent Policy Gradients. *arXiv preprint arXiv:1705.08926*, 2017.
- [7] Maximilian Hüttenrauch, Adrian Šošić, and Gerhard Neumann. Guided deep reinforcement learning for swarm systems. *arXiv preprint arXiv:1709.06011*, 2017.
- [8] Diederik P Kingma and Jimmy Ba. Adam: A method for stochastic optimization. *arXiv preprint arXiv:1412.6980*, 2014.
- [9] Landon Kraemer and Bikramjit Banerjee. Multi-agent reinforcement learning as a rehearsal for decentralized planning. *Neurocomputing*, 190:82–94, 2016. ISSN 09252312. doi: 10.1016/j.neucom.2016.01.031.
- [10] Ryan Lowe, Yi Wu, Aviv Tamar, Jean Harb, Pieter Abbeel, and Igor Mordatch. Multi-Agent Actor-Critic for Mixed Cooperative-Competitive Environments. *arXiv preprint arXiv:1706.02275*, 2020.
- [11] Anuj Mahajan, Tabish Rashid, Mikayel Samvelyan, and Shimon Whiteson. MAVEN: Multi-Agent Variational Exploration. *arXiv preprint arXiv:1910.07483*, 2020.
- [12] Volodymyr Mnih, Koray Kavukcuoglu, David Silver, Alex Graves, Ioannis Antonoglou, Daan Wierstra, and Martin Riedmiller. Playing atari with deep reinforcement learning. *arXiv preprint arXiv:1312.5602*, 2013.
- [13] Volodymyr Mnih, Adrià Puigdomènech Badia, Mehdi Mirza, Alex Graves, Timothy P. Lillicrap, Tim Harley, David Silver, and Koray Kavukcuoglu. Asynchronous Methods for Deep Reinforcement Learning. *arXiv:1602.01783*, 2016.
- [14] Sylvie CW Ong, Shao Wei Png, David Hsu, and Wee Sun Lee. Pomdps for robotic tasks with mixed observability. 5:4, 2009.
- [15] Bei Peng, Tabish Rashid, Christian A Schroeder de Witt, Pierre-Alexandre Kamienny, Philip HS Torr, Wendelin Böhmer, and Shimon Whiteson. Facmac: Factored multi-agent centralised policy gradients. *arXiv e-prints*, pages arXiv–2003, 2020.
- [16] Jing Peng and Ronald J Williams. Incremental multi-step q-learning. In *Machine Learning Proceedings 1994*, pages 226–232. Elsevier, 1994.
- [17] Doina Precup. Eligibility traces for off-policy policy evaluation. *Computer Science Department Faculty Publication Series*, page 80, 2000.
- [18] Tabish Rashid, Mikayel Samvelyan, Christian Schroeder de Witt, Gregory Farquhar, Jakob Foerster, and Shimon Whiteson. QMIX: Monotonic Value Function Factorisation for Deep Multi-Agent Reinforcement Learning. *arXiv preprint arXiv:1803.11485*, 2018.

[19] Tabish Rashid, Gregory Farquhar, Bei Peng, and Shimon Whiteson. Weighted QMIX: Expanding Monotonic Value Function Factorisation. *arXiv preprint arXiv:2006.10800*, 2020.

[20] Mikayel Samvelyan, Tabish Rashid, Christian Schroeder de Witt, Gregory Farquhar, Nantas Nardelli, Tim G. J. Rudner, Chia-Man Hung, Philip H. S. Torr, Jakob Foerster, and Shimon Whiteson. The StarCraft Multi-Agent Challenge. *arXiv preprint arXiv:1902.04043*, 2019.

[21] John Schulman, Filip Wolski, Prafulla Dhariwal, Alec Radford, and Oleg Klimov. Proximal policy optimization algorithms. *arXiv preprint arXiv:1707.06347*, 2017.

[22] Kyunghwan Son, Daewoo Kim, Wan Ju Kang, David Earl Hostallero, and Yung Yi. QTRAN: Learning to Factorize with Transformation for Cooperative Multi-Agent Reinforcement Learning. *arXiv preprint arXiv:1905.05408*, 2019.

[23] Kyunghwan Son, Sungsoo Ahn, Roben Delos Reyes, Jinwoo Shin, and Yung Yi. QTRAN++: Improved Value Transformation for Cooperative Multi-Agent Reinforcement Learning. *arXiv:2006.12010*, 2020.

[24] Adam Stooke and Pieter Abbeel. Accelerated methods for deep reinforcement learning. *arXiv preprint arXiv:1803.02811*, 2018.

[25] Jianyu Su, Stephen Adams, and Peter A Beling. Value-decomposition multi-agent actor-critics. *arXiv preprint arXiv:2007.12306*, 2020.

[26] Jianyu Su, Stephen Adams, and Peter A. Beling. Value-Decomposition Multi-Agent Actor-Critics. *arXiv:2007.12306*, 2020.

[27] Peter Sunehag, Guy Lever, Audrunas Gruslys, Wojciech Marian Czarnecki, Vinicius Zambaldi, Max Jaderberg, Marc Lanctot, Nicolas Sonnerat, Joel Z. Leibo, Karl Tuyls, and Thore Graepel. Value-Decomposition Networks For Cooperative Multi-Agent Learning. *arXiv preprint arXiv:1706.05296*, 2017.

[28] Richard S Sutton and Andrew G Barto. *Reinforcement learning: An introduction*. MIT press, 2018.

[29] Ming Tan. Multi-agent reinforcement learning: Independent vs. cooperative agents. In *Proceedings of the tenth international conference on machine learning*, pages 330–337, 1993.

[30] Jianhao Wang, Zhizhou Ren, Terry Liu, Yang Yu, and Chongjie Zhang. QPLEX: Duplex Dueling Multi-Agent Q-Learning. *arXiv:2008.01062*, 2020.

[31] Tonghan Wang, Heng Dong, Victor Lesser, and Chongjie Zhang. ROMA: Multi-Agent Reinforcement Learning with Emergent Roles. *arXiv preprint arXiv:2003.08039*, 2020.

[32] Yihan Wang, Beining Han, Tonghan Wang, Heng Dong, and Chongjie Zhang. Off-Policy Multi-Agent Decomposed Policy Gradients. *arXiv:2007.12322*, 2020.

[33] Ziyu Wang, Tom Schaul, Matteo Hessel, Hado Hasselt, Marc Lanctot, and Nando Freitas. Dueling network architectures for deep reinforcement learning. In *International conference on machine learning*, pages 1995–2003. PMLR, 2016.

[34] Ermo Wei, Drew Wicke, David Freelan, and Sean Luke. Multiagent Soft Q-Learning. *arXiv preprint arXiv:1804.09817*, 2018.

[35] Yaodong Yang, Jianye Hao, Ben Liao, Kun Shao, Guangyong Chen, Wulong Liu, and Hongyao Tang. Qatten: A General Framework for Cooperative Multiagent Reinforcement Learning. *arXiv preprint arXiv:2002.03939*, 2020.

[36] Chongjie Zhang and Victor Lesser. Coordinated multi-agent reinforcement learning in networked distributed pomdps. In *Proceedings of the AAAI Conference on Artificial Intelligence*, volume 25, 2011.

[37] Meng Zhou, Ziyu Liu, Pengwei Sui, Yixuan Li, and Yuk Ying Chung. Learning Implicit Credit Assignment for Multi-Agent Actor-Critic. *arXiv preprint arXiv:2007.02529*, 2020.

A Predator-Prey

In the vanilla Predator-Prey [10], three cooperating agents control three predators to chase a faster prey (the prey acts randomly) by controlling their velocities with actions [up, down, left, right, stop] within an area containing two large obstacles at random locations. The goal is to capture the prey with the fewest steps possible.

Predator-Prey By contrast, we use a variant of Predator-Prey from [2], which requires two predators to catch the prey at the same time to get a reward. Therefore, the variant requires effective agent coordination. However, [2] added a penalty to the agents if only one predator catches the prey (not two predators at the same time), which makes the environments somewhat competitive. The penalty requires two predators capture the prey at the same time. If a diligent predator prefers to capture the prey and the other lazy one does not ¹², then they have conflicting interests. In our experiments, we remove the penalty to ensure that the environment is purely cooperative.

Continuous Predator-Prey We also use the Continuous Predator-Prey from [15]. To obtain a hard cooperative environment, [15] replaces the prey’s policy with a hard-coded heuristic that, at any time step, moves the prey to the sampled position with the largest distance to the closest predator. Therefore, the Continuous Predator-Prey is more difficult than the Predator-prey used by MADDPG [10].

B Eligibility trace

$\text{TD}(\lambda)$ can be expressed as Eq. 5:

$$\begin{aligned} G_s^\lambda &\doteq (1 - \lambda) \sum_{n=1}^{\infty} \lambda^{n-1} G_{s:s+n} \\ G_{s:s+n} &\doteq \sum_{t=s}^{s+n} \gamma^{t-s} r_t + \gamma^{n+1} Q(s_{s+n+1}, u) \end{aligned} \tag{5}$$

$Q(\lambda)$ replaces the Q value of the next state with the max Q value, as shown in Eq. 6:

$$G_{s:s+n} \doteq \sum_{t=s}^{s+n} \gamma^{t-s} r_t + \gamma^{n+1} \max_u Q(s_{s+n+1}, u) \tag{6}$$

where λ is the discount factor of the traces and $(\prod_{s=1}^t \lambda) = 1$ when $t = 0$. When λ is set to 0, it is equivalent to 1-step bootstrap returns. When λ is set to 1, it is equivalent to Monte Carlo [28] returns.

C RIIT

RIIT decomposes training into offline and online phases; we use offline samples to train the critic network with 1-step TD error loss; then, we use the online samples to train policy networks end-to-end and critic with $\text{TD}(\lambda)$. Training policy networks with online samples improve learning stability ¹³. Furthermore, the offline training phase improves sample efficiency for critic networks. Algo. 1 demonstrates the training process of RIIT.

Algorithm 1 Optimization Procedure for RIIT

Initialize offline replay memory D and online replay memory D' .
 Randomly initialize θ and ϕ for the policy networks and the mixing critic respectively.
 Set $\phi^- \leftarrow \phi$.

while not terminated **do**

Off-policy stage

Sample b episodes τ_1, \dots, τ_b with $\tau_i = \{s_{0,i}, o_{0,i}, u_{0,i}, r_{0,i}, \dots, s_{T,i}, o_{T,i}, u_{T,i}, r_{T,i}\}$ from offline replay memory D .

Update the monotonic mixing network with $y_{t,i}$ calculated by 1-step bootstrap return ($y_{t,i} = r_{t,i} + \gamma Q_{\phi^-}^{\pi}(s_{t+1}, \vec{u}_{t+1})$):

$$\nabla_{\phi} \frac{1}{bT} \sum_{i=1}^b \sum_{t=1}^T (y_{t,i} - Q_{\phi}^{\pi}(s_{t,i}, u_{t,i}^1, \dots, u_{t,i}^n))^2. \quad (7)$$

On-policy stage

Sample b episodes τ_1, \dots, τ_b with $\tau_i = \{s_{0,i}, o_{0,i}, u_{0,i}, r_{0,i}, \dots, s_{T,i}, o_{T,i}, u_{T,i}, r_{T,i}\}$ from online replay memory D' .

Update the monotonic mixing network with $y_{t,i}^{TD(\lambda)}$ calculated by TD(λ) (Eq. 5):

$$\nabla_{\phi} \frac{1}{bT} \sum_{i=1}^b \sum_{t=1}^T (y_{t,i}^{TD(\lambda)} - Q_{\phi}^{\pi}(s_{t,i}, u_{t,i}^1, \dots, u_{t,i}^n))^2. \quad (8)$$

Update the decentralized policy networks end-to-end by maximizing the Q value, with adaptive entropy loss (Appendix E.6) :

$$\nabla_{\theta} \frac{1}{bT} \sum_{i=1}^b \sum_{t=1}^T \left(Q_{\phi}^{\pi}(s_{t,i}, \pi_{\theta_1}^1(\cdot|z_{t,i}^1), \dots, \pi_{\theta_n}^n(\cdot|z_{t,i}^n)) + \frac{1}{n} \sum_{a=1}^n \mathcal{H}(\pi_{\theta_a}^a(\cdot|z_{t,i}^a)) \right). \quad (9)$$

if at target update interval **then**

Update the target mixing network $\phi^- \leftarrow \phi$.

end if

end while

Algorithms	Value-based (VB)	Policy-bassed (PG)
Optimizer	Adam, RMSProp	Adam, RMSProp
Learning Rates	0.0005, 0.001	0.0001 (for DOP), 0.0005, 0.001,
Batch Size(episodes)	32, 64, 128	32, 64
Replay Buffer Size	5000, 10000, 20000	2000, 5000, 10000, 20000
Q(λ), TD(λ)	0, 0.3, 0.6, 0.9	0, 0.3, 0.6, 0.9
Adaptive Entropy	-	0.01, 0.03, 0.06, (add 0.0005, 0.0001, 0.001 for DOP)
ϵ Anneal Steps	50K, 100K, 500K, 1000K	-

Table 5: Hyperparameters Search on 5m_vs_6m and 3s5z_vs_3s6z.

D Experiments Details

D.1 Hyperparameters

As shown in Table 5, we perform grid search schemes on a typical hard environment (5m_vs_6m) and super hard environment (3s5z_vs_3s6z) to find a **general** set of hyperparameters for each algorithm. The reason why we avoid careful tuning of the hyperparameters for all scenarios is that robustness is also important for MARL algorithms. It is worth stating that our hyperparameter search scope contains whether to use a trick, e.g. setting λ to 0 is equivalent to the 1-step TD algorithm.

¹²Because reinforcement learning algorithms explore randomly, some samples with penalized rewards can cause certain agents to tend to be lazy.

¹³[4] shows that actor networks generally have a lower tolerance for sample reuse than critic networks

Algorithms	LICA	OurLICA	DOP	OurDOP	RIIT
Optimizer	Adam	Adam	RMSProp	Adam	Adam
Batch Size(episodes)	32	32	Off=32, On=16	Off=64, On=32	Off=64, On=32
TD(λ)	0.8	0.6	0.8, TB($\lambda=0.93$)	0.6, TB($\lambda=0.9$)	0.6
Adaptive Entropy	0.06	0.06	-	0.0005	0.03
ϵ Anneal Steps	-	-	500K	-	-
Critic-Net Size	29696K	208K	122K	122K	69K
Rollout Processes	32	8	4	8	8

(a) Setting of Policy-based algorithms.

Algorithms	QMIX	OurQMIX	Qatten	OurQatten	QPLEX	OurQPLEX
Optimizer	RMSProp	Adam	RMSProp	Adam	RMSProp	Adam
Batch Size (epi.)	128	128	32	128	32	128
Q(λ)	0	0.6	0	0.6	0	0.6
Attention Heads	-	-	4	4	10	4
Mixing-Net Size	41K	41K	58K	58K	476K	152K
ϵ Anneal Steps			50K \rightarrow 500K for 6h_vs_8z, 100 K for others			
Rollout Processes	8	8	1	8	1	8

(b) Setting of Value-based algorithm.

Table 6: Hyperparameters Settings.

Based on the results of the grid search, we further explain how these hyperparameters are set. Table 6a and 6b shows our general settings for the these algorithms. The network size is calculated under 6h_vs_8z, where adding *Our* denotes the new hyperparameter settings.

Neural Network Size We first ensure the network size is the same order of magnitude, which means that we decrease the critic-net size of LICA from 29696K to 208K, and we use 4 attention heads leading the mixing-net size of QPLEX from 476K to 152K. All the agent networks are the same as those found in QMIX [18].

Optimizer & Learning Rate We use Adam to optimize all networks as Adam may accelerate the convergence of the algorithms. Furthermore, we use different learning rates for each algorithm: (1) For all value-based algorithms, neural networks are trained with 0.001 learning rate. (2) For LICA, we set the learning rate of the agent network to 0.0025 and the critic network’s learning rate to 0.0005. (3) For DOP, we set the agent network’s learning rate to 0.0005 and the learning rate of the critic network to 0.0001. (4) For RIIT, we set the learning rates to 0.001.

Batch Size We find that a large batch size helps to improve the stability of the algorithms. Therefore, for value-based algorithms, we set the batch size to 128. For the policy-based algorithms, we set the batch size to 64/32 (Offline/Online training) due to the fact that online sample requires only the newest data.

Replay Buffer Size As discussed in Sec. 5.1.3, a small replay buffer size facilitates the convergence of the MARL algorithms. Therefore, for SMAC, the size of all replay buffers is set to 5000 episodes. For Predator-Prey, we set the buffer size to 1000 episodes.

Exploration As discussed in Sec. 5.1.5, we use ϵ -greedy action selection, decreasing ϵ from 1 to 0.05 over n-time steps (n can be found in Table 6b) for value-based algorithms. We use the Adaptive Entropy (Appendix. E.6) for all policy-based algorithms because it facilitates the automatic adjustment of the size of the entropy loss in different scenarios. We also add the Adaptive Entropy to DOP to prevent DOP from crashing.

TD(λ) Since replay buffer size and ϵ are set to small values, the convergence of TD(λ) is guaranteed. We find that the value of TD(λ) is closely related to the test scenarios. We are using $\lambda = 0.6$ for all tasks as the value works stably in most scenarios.

Rollout Processes Number Eight rollout processes for parallel sampling are used to obtain as many samples as possible from the environments at a high rate. This also ensures that all the algorithms share the same number of policy iterations and sample size (10 million).

Other Settings We set all discount factors $\gamma = 0.99$. We update the target network every 200 episodes. We do not reshape the reward of SMAC and Predator-Prey, as they provide a default shaping reward. We use StarCraft 2 Version B75689 (SC2.4.10) in our experiments. We find that the optimal hyperparameters of the value-based algorithms are similar due to the fact that they share the same basic architecture and training paradigm. Therefore, the settings for VDNs and WQMIX are the same as for QMIX. Specifically, we use OW-QMIX, detailed in E.5, in WQMIX as the baseline.

D.2 Omitted Figures

We echo our experiments in Sec. 5.2.1. We provide detailed experiment results to support our core statements. Figure 9 and 8 shows that QMIX achieves excellent performance on all Hard Scenarios in SMAC. Figure 9 shows that QPLEX’s policy collapses in the test of Super Hard 6h_vs_8z and corridor¹⁴. Figure 10 and Table 4 show that each of the algorithms achieves good performance on cooperative Predator-Prey.

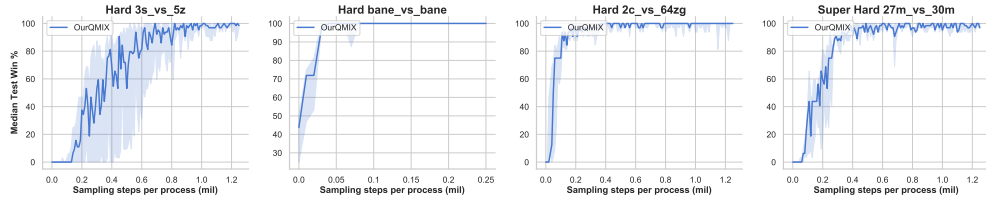


Figure 8: Median test win rate of OurQMIX on Hard Scenarios in SMAC.

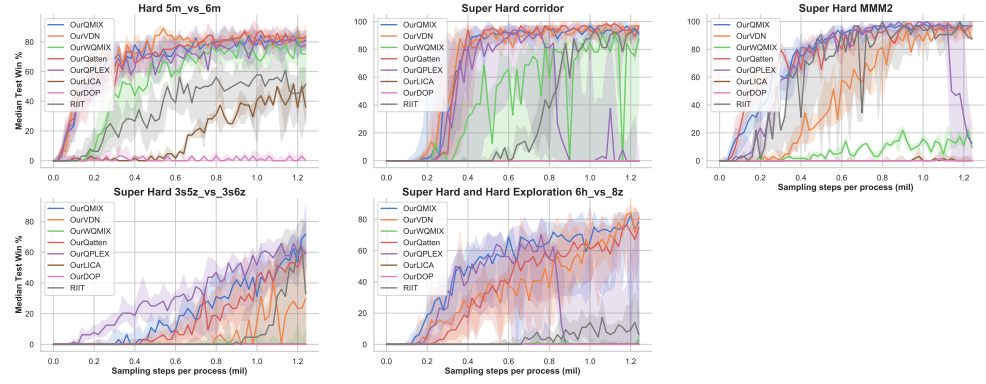


Figure 9: Median test win rate of MARL algorithms on SMAC.

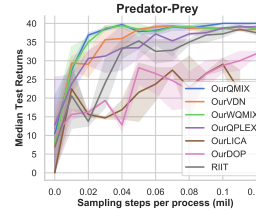


Figure 10: Median episode return of MARL algorithms on Predator-Prey (Appendix A).

D.3 Comparing with Original Algorithm

In this section, we make a simple horizontal comparison for the original algorithms. We compare their original performance with third-party experimental results, i.e. experimental results of the paper citing the algorithm.

¹⁴It may be that QPLEX feeds both actions and states into the mixing network in its implementation. The mixing network can predict true Q_{tot} without correct Q_i , so that the Q_i becomes useless.

For VDNs and QMIX, the original SMAC paper [20] shows that VDNs and QMIX do not perform well in hard and super hard scenarios. For Qatten, the experiments in [30] demonstrates that the performance of Qatten is worse than vanilla QMIX. [15] demonstrates that QPLEX and DOP does not work well in hard and super hard scenarios in SMAC, and the performance of DOP is worse than QMIX. It is interesting that WQMIX [19] shows the poor performance of WQMIX in super hard scenarios *3s5z_vs_3s6z* and *corridor*. The original test results in LICA are not considered as 64 million samples are used in their experiments.

However, after our hyperparameter tuning, all the value-based methods achieve good performance in Hard and Super Hard scenarios. Therefore, *Our* method, i.e. OurVDNs, OurQatten, OurQPLEX, OurWQMIX have better performance than the original ones.

E Cooperative MARL

E.1 IQL

Independent Q-learning (IQL) [29] breaks down a multi-agent task into a series of simultaneous single-agent tasks that share the same environment, just like multi-agent Deep Q-networks (DQN) [12]. DQN represents the action-value function with a deep neural network parameterized by θ . DQN uses a replay buffer to store transition tuple $\langle s, u, r, s' \rangle$, where state s' is observed after taking action u in state s and obtaining reward r . However, IQL does not address the non-stationarity introduced due to the changing policies of the learning agents. Thus, unlike single-agent DQN, there is no guarantee of convergence even at the limit of infinite exploration.

E.2 VDNs

By contrast, Value decomposition networks (VDNs)¹⁵ [27] seek to learn a joint action-value function $Q_{tot}(\tau, \mathbf{u})$, where $\tau \in \mathbf{T} \equiv \mathcal{T}^n$ is a joint action- observation history and \mathbf{u} is a joint action. It represents Q_{tot} as the sum of individual value functions Q_a ($\tau^i, u^i; \theta^i$):

$$Q_{tot}(\tau, \mathbf{u}) = \sum_{i=1}^n Q_i(\tau^i, u^i; \theta^i).$$

E.3 Qatten

Qatten¹⁶ [35], introduces an attention mechanism into the monotonic mixing network of QMIX:

$$Q_{tot} \approx c(s) + \sum_{h=1}^H w_h \sum_{i=1}^N \lambda_{i,h} Q^i \quad (10)$$

$$\lambda_{i,h} \propto \exp(e_i^T W_{k,h}^T W_{q,h} e_s) \quad (11)$$

where $w_h = |f^{NN}(s)|_h$, $W_{q,h}$ transforms e_s into a global query, and $W_{k,h}$ transforms e_i into an individual key. The e_s and e_i may be obtained by an embedding transformation layer for the true global state s and the individual state s_i .

E.4 QPLEX

QPLEX¹⁷ [30] decomposes Q values into advantages and values based on Qatten, similar to Dueling-DQN [33]:

$$\begin{aligned} \text{(Joint Dueling)} \quad Q_{tot}(\tau, u) &= V_{tot}(\tau) + A_{tot}(\tau, u) \\ V_{tot}(\tau) &= \max_{u'} Q_{tot}(\tau, \mathbf{u}') \end{aligned} \quad (12)$$

¹⁵VDN code: <https://github.com/oxwhirl/pymarl>

¹⁶Qatten code: <https://github.com/simsimiSION/pymarl-algorithm-extension-via-starcraft>

¹⁷QPLEX code: <https://github.com/wjh720/QPLEX>

$$\begin{aligned}
\text{(Individual Dueling)} \quad & Q_i(\tau_i, u_i) = V_i(\tau_i) + A_i(\tau_i, u_i) \\
& V_i(\tau_i) = \max_{u'} Q_i(\tau_i, u'_i)
\end{aligned} \tag{13}$$

$$\frac{\partial A_{tot}(s, \mathbf{u}; \boldsymbol{\theta}, \phi)}{\partial A_i(\tau^i, u^i; \theta^i)} \geq 0, \quad \forall i \in \mathcal{N} \tag{14}$$

In other words, Eq. 14 (advantage-based monotonicity) transfers the monotonicity constraint from Q values to advantage values. QPLEX thereby reduces limitations on the mixing network's expressiveness.

E.5 WQMIX

WQMIX¹⁸ [19], just like Optimistically-Weighted QMIX (OW-QMIX), uses different weights for each sample to calculate the squared TD error of QMIX:

$$\mathcal{L}(\theta) = \sum_{i=1}^b w(s, \mathbf{u}) (Q_{tot}(\boldsymbol{\tau}, \mathbf{u}, s) - y_i)^2 \tag{15}$$

$$w(s, \mathbf{u}) = \begin{cases} 1 & Q_{tot}(\boldsymbol{\tau}, \mathbf{u}, s) < y_i \\ \alpha & \text{otherwise.} \end{cases} \tag{16}$$

Where $\alpha \in (0, 1]$ is a hyperparameter and y_i is the true target Q value. WQMIX prefers those optimistic samples (true returns are larger than predicted), i.e., decreasing the weights of samples with non-optimistic returns. More critically, WQMIX uses an unconstrained true Q Network as a target network to guide the learning of QMIX. The authors prove that this approach can resolve the estimation errors of QMIX in the non-monotonic case.

E.6 LICA

LICA¹⁹ [37] completely removes the monotonicity constraint through a policy mixing critic, as shown in Figure 11:

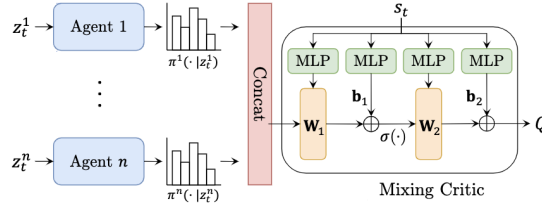


Figure 11: Architecture for LICA (from [37]). LICA's mixing critic maps policy distribution to the Q value directly, in effect obviating the monotonicity constraint. z denotes local action observation history.

LICA's mixing critic is trained using squared TD error. With a trained critic estimate, decentralized policy networks may then be optimized end-to-end simultaneously by maximizing $Q_{\theta_c}^\pi$ with the stochastic policies $\pi_{\theta_i}^i$ as inputs:

$$\max_{\theta} \mathbb{E}_{t, s_t, u_t^1, \dots, \tau_t^n} [Q_{\theta_c}^\pi(s_t, \pi_{\theta_1}^1(\cdot | \tau_t^1), \dots, \pi_{\theta_n}^n(\cdot | \tau_t^n)) + \mathbb{E}_i [\mathcal{H}(\pi_{\theta_i}^i(\cdot | \tau_t^i))]] \tag{17}$$

where the gradient of entropy item $\mathbb{E}_i [\mathcal{H}(\pi_{\theta_i}^i(\cdot | z_t^i))]$ is normalized by taking the quotient of its own modulus length: Adaptive Entropy (Adapt Ent). Adaptive Entropy automatically adjusts the coefficient of entropy loss in different scenarios.

¹⁸WQMIX code: <https://github.com/oxwhirl/wqmix>

¹⁹LICA code: <https://github.com/mzho7212/LICA>

E.7 VMIX

VMIX²⁰ [25] combines the Advantage Actor-Critic (A2C) [24] with QMIX to extend the monotonicity constraint to value networks (not Q value network), as shown in Eq. 19. We verified that the monotonicity constraint also has a positive effect on the value network based on VMIX (Figure 7).

$$V_{tot}(s; \theta, \phi) \\ = g_\phi(s, V^1(\tau^1; \theta^1), \dots, V^N(\tau^N; \theta^N)) \quad (18)$$

$$\frac{\partial V_{tot}}{\partial V^i} \geq 0, \quad \forall i \in \{1, \dots, N\} \quad (19)$$

where ϕ is the parameter of value mixing network, and θ_i is the parameter of agent network. With the centralized value function V_{tot} , the policy networks can be trained by policy gradient (Eq. 20),

$$\hat{g}_i = \frac{1}{|\mathcal{D}|} \sum_{\tau \in \mathcal{D}} \sum_{t=0}^T \nabla_\theta \log \pi_{\theta^i}(u_t^i | \tau_t^i) \Big|_{\theta^i} \hat{A}_t \quad (20)$$

where $\hat{A}_t = r + V_{tot}(s') - V_{tot}(s)$ is the advantage function, and \mathcal{D} denotes replay buffer.

E.8 Relationship between previous works

VDNs requires a linear decomposition of Q values, so it has the strongest monotonicity constraint. Since the weights calculated by softmax (attention mechanism) are greater than or equal to zero, Qatten and QMIX share the same constraint strength. QPLEX just shifts the constraint to advantage values without removing it. WQMIX relaxes the monotonicity constraint even further by a true Q value network and theoretical guarantees. LICA completely removes the monotonicity constraint by new network architecture. We rank the strength of the monotonicity constraints on these MARL algorithms:

$$VDNs > QMIX = Qatten > QPLEX > WQMIX > LICA.$$

²⁰VMIX code: <https://github.com/hahayonghuming/VDACs>